J Mater Sci (2007) 42:328–331
DOI 10.1007/s10853-006-1028-1

Microstructure and characterization of phases in TIG welded joints of Zircaloy-4 and stainless steel 304L

M. Ahmad · J. I. Akhter · M. Akhtar · M. Iqbal

Received: 27 July 2004 / Accepted: 30 August 2005 / Published online: 22 November 2006

Abstract Tungsten inert gas (TIG) welded joints between Zircaloy-4 and stainless steel 304L have been studied by scanning electron microscope (SEM) having energy dispersive system (EDS) as an attachment. Intermetallic compound $Zr(Cr, Fe)_2$ and Zr_2Fe–Zr_2Ni eutectic phase have been observed in the molten zone. The surface area occupied by intermetallic compound $Zr(Cr, Fe)_2$ is about twice compared to Zr_2Fe–Zr_2Ni eutectic phase. The shape of the intermetallic compound is rod like. The phases were also identified by using X-ray diffraction (XRD) technique. EDS and XRD results are quite in agreement.

Introduction

Zircaloy-4 is used as cladding material for fuel element in nuclear thermal reactors due to its several attractive properties like low neutron absorption cross-section, excellent corrosion resistance and good mechanical properties at elevated temperature [1]. Stainless steel is used as a structural material in nuclear reactors. The interaction of these materials could take place in case of an accident when temperature is raised suddenly. The interactions between stainless steel and Zircaloy have been studied by many authors in the past and results have been published in the literature [2–6]. These interactions between stainless steel-304L and Zircaloy-4 were produced by solid state diffusion bonding. Mukherjee and Panakkal [7] studied interaction occurred between SS-302 spring and Zircaloy-4 during TIG welding of small diameter experimental nuclear fuel pin and correlated high hardness of the diffusion zone with the formation of intermetallics. However, composition and density of the phases were not reported. Formation of defects, i.e., cracks/microcracks and microfissures were also observed. The morphology, structure and hardness of different phases in the welded region were remained unknown.

Ahmad et al. [8] characterized the phases formed in the molten zone of electron beam welded joint of Zircaloy-4 and stainless steel 304L and observed reduction in the brittle intermetallic $Zr(Cr, Fe)_2$, the main phase responsible for the nucleation of cracks. Zhou and Zhou [9] studied the microstructure of explosive welded joints of Zircaloy-4 and stainless steel and observed the only crystalline phase $Zr(Cr, Fe)_2$ with hexagonal structure and concluded that welded joints could be bent and rolled without crack formation. Kleykamp and Pejsa [10] observed different phases while studying the samples taken from the molten core region of the damaged Three Miles Island-2 (TMI-2) reactor.

Welding is very important process for manufacturing the components and parts of different materials. TIG welding is commonly applied in most of the structures. There is only one report on TIG welding of dissimilar/incompatible materials like Zircaloy-4 and stainless steel 302, which did not confirm type, structure of phases, their shape and relative density. The aim of the present investigation is to study the detailed microstructure, phases and morphology of the molten zone and heat affected zones (HAZs) of the TIG

M. Ahmad (✉) · J. I. Akhter · M. Akhtar · M. Iqbal
Physics Research Division, Pakistan Institute of Nuclear Science & Technology, P.O. Nilore, Islamabad, Pakistan
e-mail: maqomer@yahoo.com

Table 1 Nominal composition of alloys

Alloy	Elements in wt%							
	Sn	Cr	Ni	Si	C	Mn	Fe	Zr
Zircaloy-4	1.52	0.10	<0.005	–	0.002	–	0.20	bal.
Stainless steel 304L	–	19.0	10.00	1.0	0.03	2.0	bal.	–

welded joints of the Zircaloy-4 and stainless steel 304L and to characterize the phases by EDS and XRD and their effect on the microhardness.

Experimental

The nominal composition of both the alloy is given in Table 1. Samples of the size $2 \times 1 \times 0.3$ cm^3 were cut from the sheet of 304L and Zircaloy-4. Joining sides of both the alloys were polished on lapping machine using the diamond paste down to 0.25 μm. Butt joints were made using the TIG welding technique. The filler metal used for welding was stainless steel 304L. The TIG welding was performed using machine voltage of 30–60 V and current 12–15 A. The flow of Ar gas was 15 l/min. The welding time was about 60 s. After TIG welding the samples were polished and etched chemically in a solution of H_2O_2:HNO_3:HF with a volume ratio of 6:6:1. The microstructure of the molten zone was investigated by scanning electron microscope (SEM) and the composition of the phases were determined using the energy dispersive system (EDS) attached with SEM. Phases were also identified with XRD using Cu$K\alpha$1 line $\lambda = 1.54051$ Å. Microhardness values of different phases were measured using a load of 1.96 N at room temperature.

Results and discussion

SEM micrograph with secondary electron image (SEI) of the molten zone is shown in Fig. 1, which indicates two distinct phases. Backscattered electron image (BEI) for composition, shown in Fig. 2 at high magnification, also clearly reveals two phases. Point analysis of these phases indicates that one phase is rich in Zr, Fe and Ni and the other is enriched in Zr, Cr and Fe. The concentration of these elements varies from point to point and the average content of several points is given in Table 2. The tentative phase diagrams of the ternary systems Zr–Fe–Cr and Zr–Fe–Ni, given in the literature [10] at 1000 °C, are shown in Fig. 3. Our composition of the Zr, Cr and Fe enriched phase corresponds to the phase Zr(Cr, Fe)$_2$ and Zr, Fe, Ni,

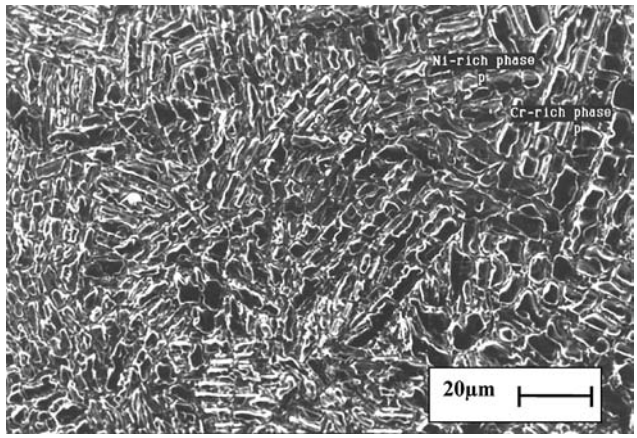

Fig. 1 SEM micrograph (secondary electron image) showing

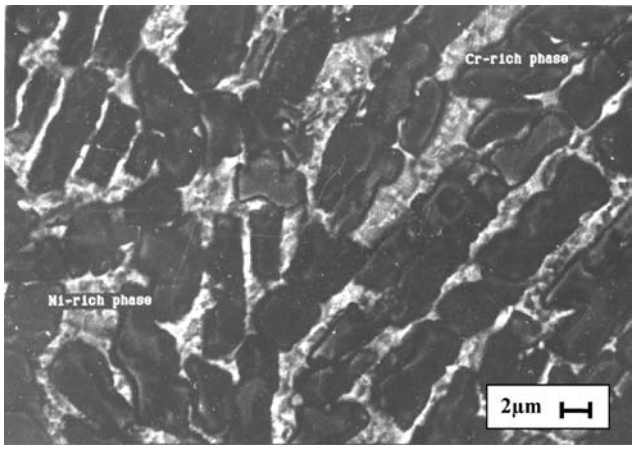

Fig. 2 SEM micrograph (backscattered electron image) at high magnification, which clearly indicates different phases in molten zone

Table 2 Quantitative X-ray analysis of phases in molten zone of TIG welded Zircaloy-4 and stainless steel 304L

	Phases	Elements (wt %)						
		Cr	Fe	Zr	Ni	Sn	Si	Mn
Molten zone	Zr (Cr, Fe)$_2$	15.03	33.78	49.50	1.67	–	–	–
	Zr_2Fe–Zr_2Ni	2.20	14.26	77.18	6.21	–	–	–
Heat affected zones	Zircloy-4 side	1.30	10.24	84.36	2.02	2.08	–	–
	SS 304L side	19.36	67.32	1.0	9.84	–	0.78	1.71

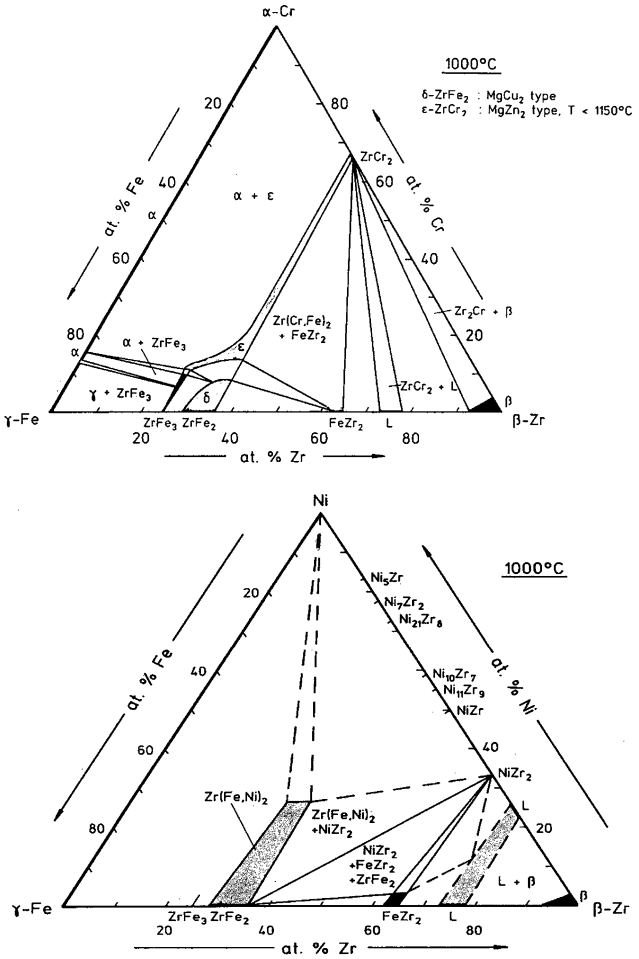

Fig. 3 Tentative phase diagrams of Zr–Fe–Cr (above) and Zr–Fe–Ni (below) [10]

rich phase correspond to Zr_2Fe–Zr_2Ni eutectic phase. These phases have already been characterized by [8] in the molten zone of the electron beam welded specimens of Zircaloy-4 and SS-304L. The density of the intermetallic compound $Zr(Cr, Fe)_2$ in the molten zone is about twice that of Zr_2Fe–Zr_2Ni eutectic phase in the TIG welded specimen. On the other hand the intermetallic compound $Zr(Cr, Fe)_2$ was observed only in the region formed in the molten zone near stainless steel and Zr_2Fe–Zr_2Ni eutectic in rest of the molten zone with dendritic structure in EBW specimen [8]. The dendritic structure is believed to create higher solidification cracking resistance [11]. The hardness values of the $Zr(Cr, Fe)_2$ is about three times higher compared to the hardness value of Zr_2Fe–Zr_2Ni eutectic phase. These microhardness values are in good agreement with the values already measured for these phases by Ahmad et al. [8] in case of electron beam welding. The density of the $Zr(Cr, Fe)_2$ is low near the Zircaloy-4 side compared to rest of the molten

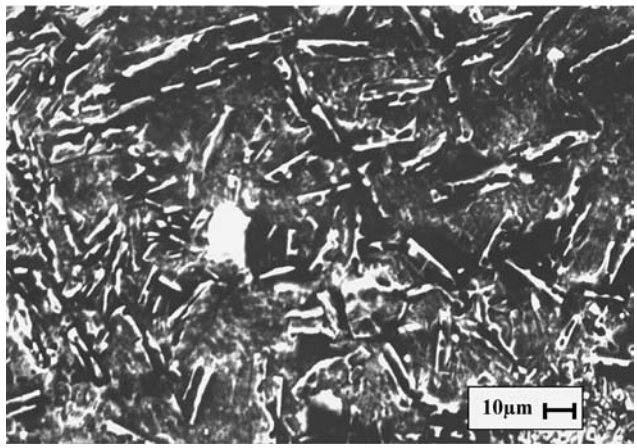

Fig. 4 SEM micrograph (secondary electron image) showing the density of the phase Zr $(Cr, Fe)_2$ near the Zircaloy-4

zone. SEM micrograph showing the density of the $Zr(Cr, Fe)_2$ in the fusion zone, very near to Zircaloy-4, is shown in Fig. 4. The reason of low density in this area is the less availability of Cr and Fe and more availability of Zr. A Cr rich and Ni depleted region or layer is not observed in the HAZs in the stainless steel that the authors [8, 12] observed on the side of stainless steel 304L in the joints of Zircaloy-4 and stainless steel 304L produced by electron beam welding and diffusion bonding. The composition of the HAZs is given in Table 2, which also shows minute change in the concentration of Ni and Cr compared with the nominal composition of the SS 304L. This may be due to the fact that the diffusion of Fe, Ni and Cr has been taking place from the filler material towards the stainless steel and Zircaloy-4 and also diffusion of Fe, Cr and Ni has been taking place from the large area of the heat affected region in the stainless steel 304L. HAZ near the fusion zone in stainless steel contains very small amounts of Zr and Sn and HAZ near the molten zone in Zircaloy-4 also contains small quantity of Cr, Ni and Fe. The width of the HAZ is about 0.1 mm in both the alloys from the molten zone. Grain growth is observed in HAZ on both sides of the molten zone. In order to confirm the identified phases on the basis of quantitative X-ray analysis of EDS spectra, XRD pattern was taken and analyzed. XRD analysis of the molten zone and HAZ, along with the data existing in the literature [5] for diffusion bonded couple of Zircaloy-2 and stainless steel and taken from JCPD cards is given for comparison in Table 3. XRD results show the presence of the $Zr(Cr, Fe)_2$, Zr_2Fe and Zr_2Ni, Zr–Fe–Ni phases along with α-Zr phase. The Phase Zr–Fe–Ni is present in the vicinity of the molten zone in the Zircaloy-4, which is already indicated by the EDS analysis, i.e., Fe, Ni and Cr are observed in Zircaoly-4 in the HAZ.

Table 3 X-ray diffraction data analysis of the TIG welded Zircaloy-4 and stainless steel 304L

d_{hkl} (Å)	Identification	*hkl*	d_{hkl}* (Å)	d_{hkl}** (Å)
2.799	Zr_2Fe	002	2.79	2.8
	α-Zr	100		2.798
2.773	Zr–Fe–Ni	002	2.772	(2.711)
2.583	Zr–Fe–Ni	211	2.577	(2.58)
	α-Zr	002		2.573
2.463	α-Zr	101	2.457	2.459
2.342	$Zr(Cr, Fe)_2$	103	–	2.311
2.247	Zr_2Ni	112	2.269	2.278
	Zr_2Fe	220		2.25
2.146	$Zr(Cr, Fe)_2$	–	2.136	2.136
2.092	$Zr(Cr, Fe)_2$	112		2.096
2.072	Zr_2Fe	310	2.052	2.046
	$Zr(Cr, Fe)_2$	202,310		2.0488
1.949	$Zr(Cr, Fe)_2$	004	–	1.916
	α-Zr	202	–	
1.894	Zr–Fe–Ni	102	1.886	(1.894)
1.794	Zr–Fe–Ni	222	1.773	(1.772)
1.664	Zr–Fe–Ni	312	1.654	(1.654)
1.612	α-Zr	110	1.613	1.616
1.544	Zr_2Fe	213	1.548	1.56
1.511	Zr–Fe–Ni	411	1.518	(1.52)
1.458	α-Zr	103	1.461	1.463
	Zr–Fe–Ni	420		(1.458)
1.436	Zr_2Fe	420	1.43	1.42
1.415	$Zr(Cr, Fe)_2$	213		1.405
1.387	α-Zr	200	–	1.399
1.365	$Zr(Cr, Fe)_2$	302	–	1.363
1.346	$NiZr_2$	322	–	1.322
1.321	$NiZr_2$	332	–	1.332
1.267	$Zr(Cr, Fe)_2$	220	–	1.252
1.179	$NiZr_2$	521	–	1.174

d_{hkl}—values measured in the present study

d_{hkl}*—values taken from [5] for the diffusion layer located in the proximity of Zircaloy-2

d_{hkl}**—values given in JCPD cards have been used. The given d_{hkl}** in parenthesis for Zr–Fe–Ni have been indexed on the basis of a body centered tetragonal cell with $a = 6.51$ Å and $c = 5.54$ Å by [5]

The slight variation in the measured d_{hkl} values from the literature may be due to the small variation in the concentration of various elements. XRD results are in good agreement with the EDS results.

Conclusions

$Zr(Cr, Fe)_2$ intermetallic compound and Zr_2Fe–Zr_2Ni eutectic phases have been observed in the molten zone of the TIG welded joints of the Zircaloy-4 and stainless steel 304L. The density of $Zr(Cr, Fe)_2$ is about twice as compared to Zr_2Fe–Zr_2Ni eutectic phase. Hardness of the $Zr(Cr, Fe)_2$ intermetallic compound is about three times higher compared to Zr_2Fe–Zr_2Ni eutectic phase. Density of $Zr(Cr, Fe)_2$ intermetallic compound is low on the side of Zircaloy-4 as compared to stainless steel 304L.

References

1. Asundi MK, Banerjee S (1989) Mater Sci Fourm 48–49:201
2. Perona G, Sesini R, Icodemi WN, Zoja R (1966) J Nucl Mater 18:278
3. Shaaban HI, Hammad FH, Baron JL (1978) J Nucl Mater 71:277
4. Bhanumurthy K, Krisknan J, Kale GB, Banerjee S (1994) J Nucl Mater 217:67
5. Lucuta PGr, Patru I, Vasiliu F (1981) J Nucl Mater 99:154
6. Shaaban HI, Hammad FH (1978) J Nucl Mater 78:431
7. Mukherjee D, Panakkal JP (1995) J Mater Sci Lett 14:1383
8. Ahmad M, Akhter JI, Shaikh MA, Akhter M, Iqbal M, Chaudhry MA (2002) J Nucl Mater 301:118
9. Zhou H, Zhou B (1996) Report CNIC-01108, SINRE-0067
10. Kleykamp H, Pejsa R (1991) Report KFK-No. 4872
11. Kim HT, Nam SW, Hwang SH (1996) J Mater Sci 31:2859
12. Ahmad M, Akhter JI, Zaman Q, shaikh MA, Akhter M, Iqbal M, Ahmed E (2003) J Nucl Mater 317:212